Direct Observation of Confined Acoustic Phonons in the Photoluminescence Spectra of a Single CdSe-CdS-ZnS Core-Shell-Shell Nanocrystal

Gerwin Chilla, Tobias Kipp,* Torben Menke, and Detlef Heitmann
Institut für Angewandte Physik und Zentrum für Mikrostrukturforschung, Universität Hamburg, Jungiusstraße 11, 20355 Hamburg, Germany

Marija Nikolic, Andreas Frömsdorf, Andreas Kornowski, Stephan Förster, and Horst Weller
Institut für Physikalische Chemie, Universität Hamburg, Grindelallee 117, 20146 Hamburg, Germany
(Received 4 October 2007; published 5 February 2008)

We report on the direct observation of confined acoustic phonons in the photoluminescence spectra of single CdSe-CdS-ZnS nanocrystals, whose ligands were exchanged to poly(ethylene oxide) (PEO) before they were embedded in a PEO matrix. Modeling a nanocrystal as an elastic sphere, the confined acoustic modes can be assigned to purely radial vibrations: the breathing mode and its two first radial harmonics. In addition to acoustic modes, we also observe longitudinal optical modes of the core material and, remarkably, also of both shell materials.

DOI: 10.1103/PhysRevLett.100.057403 PACS numbers: 78.67.Bf, 63.22.−m, 78.55.Et

Semiconductor nanocrystals (NCs), and especially their optical properties, have been intensively investigated recently because of their applications in optoelectronics and biology. The confinement of carriers inside a NC leads to discrete electronic states and an atomiclike behavior of its luminescence. The growth of larger band-gap semiconductors as shells around a lower band-gap material core leads to a significant luminescence enhancement [1,2]. Because of trap states, the surface and also the near surrounding of a NC are discussed to play a significant role regarding temporal intermittency and spectral wandering of the luminescence. A further important factor that determines the optical properties of NCs is the interaction of confined carriers with phonons. In NCs also the phonon modes become discrete due to the small dimensions. The relatively strong coupling of excitons and LO phonons via the Fröhlich interaction leads to discrete phonon replica in the emission spectra of NCs, observable also in single NC luminescence [3,4]. Acoustic phonons are of special interest since they are discussed to play an important role in the nonradiative interband relaxation of excited carriers and in line width broadening of the radiative recombination. Confined acoustic phonon modes in NCs have been detected by means of Raman spectroscopy [5–8], spectral hole-burning spectroscopy [9–11], resonant high-resolution photoluminescence spectroscopy [12] and femtosecond pump-and-probe spectroscopy [13–15]. In all these experiments an ensemble of NCs has been investigated.

In this Letter, we report the direct observation of confined acoustic phonons in the PL spectra of a single NC. This was made possible by investigating core-shell-shell CdSe-CdS-ZnS NCs whose ligands were exchanged to poly(ethylene oxide) (PEO) and who were embedded in a PEO matrix. These NCs showed strong and durable PL even under high power excitation. By using Lamb's theory on the vibrations of an elastic sphere [16], we can assign the acoustic phonon modes to radial vibrations: the breathing mode and its two first spatial harmonics.

Our CdSe-CdS-ZnS NCs were synthesized using the ''greener'' approach described in Refs. [17,18]. X-ray diffraction patterns of similar NCs show that the wurtzite phase of CdSe cores carries through to the shells [18]. The size of the core has been determined both directly by transmission electron spectroscopy and indirectly from the first absorption maximum position (2.20 eV at room temperature) using a calibration curve for CdSe NCs given in Ref. [19] which delivers an average diameter of about 3.3 nm. Calculations of the mass balance of Cd (S) in the case of CdS (ZnS) yield thicknesses of about 0.6 and 1 monolayer (ML) for the CdS and ZnS shell, respectively. Assuming a ML thickness of 0.35 nm leads to an average overall diameter of about 4.4 nm. The original Tri-*n*-octylphosphine/Tri-*n*-octylphosphine oxide (TOP/TOPO) ligands have been changed with amino-functionalized PEO ligands (PEO2000-DETA), as described in Ref. [20]. For the polymer matrix, 0.05 wt % of PEO ($M_w = 100\,000$) was dissolved in 4 ml of a toluene/chloroform mixture (2:1), stirred for 2 h, and filtered by 0.45 μm Millipore membranes. Then, 15 μl of ligand exchanged NCs ($c \approx 10^{-6}$ mol/dm^3) dissolved in chloroform were added and stirred for 20 min. The resulting solution was spin coated at 3000 rpm on polished Si(111) surfaces.

Single NCs were investigated in a micro PL setup. The sample was mounted in a cryostat and cooled to $T = 8$ K. The exciting solid state cw laser ($\lambda = 532$ nm) was focussed onto the sample by a microscope objective ($\times 80$, 0.75 NA) to a spot size of about 1 μm. The emitted light was collected by the same objective and then spectrally analyzed by a triple-grating spectrometer and detected by a CCD camera.

Figure 1 shows a PL spectrum of a single NC obtained with an excitation power of $P_{exc} = 2.5$ mW during $t_{int} = 1$ s integration time. A sharp peak at 2.1124 eV is observed arising from the recombination of an electron and a hole out of their ground states. This peak is called zero-phonon line (ZPL). Its line width of 220 μeV is resolution limited (see right inset). The left inset shows an ensemble PL spectrum of the investigated NCs before change of ligands. The ensemble emission is centered at about 2.145 eV with a width of about 60 meV. We assign the center emission energy of the ensemble to NCs with the average core diameter of 3.3 nm. The NC of Fig. 1 is redshifted by 33 meV compared to the ensemble. In order to estimate the diameter of this particular NC we assume that also its room temperature absorption would red shift by the same amount. With that we calculate as described above the core diameter of the particular NC to be 3.6 nm. This leads to an overall diameter of about 4.7 nm.

The emission of the NC of Fig. 1 has been monitored over a time period of more than five hours, exciting with different laser powers. It was found to be very stable over the whole time. In the following we will concentrate on this NC, even though we found different NCs exhibiting similar stability and showing similar results as discussed in the following. Nevertheless, not all NCs on the sample showed the same stability, often a NC was first highly luminescent but after some seconds or minutes it changed into a permanently dark NC. Since the passivating shells and the ligands of a NC strongly influence its photostability [1,2,18], one may attribute this behavior to NCs exhibiting slight inhomogeneities in their shell structure or in their surrounding polymer matrix. Important features of the temporal evolution of the emission of the NC can be deduced from Fig. 2. In each plot (a),(c),(e) the PL intensity of a series of 100 consecutively measured spectra is encoded in a gray scale. The neighboring graph of each series exemplarily depicts the spectrum at $t = 45$ s. In Fig. 2(a) the ZPL is at $E_{ZPL} = 2.1124$ eV exhibiting only a very small jitter (± 300 μeV). The most striking feature of this depiction is the visibleness of further lines on the low-energy side of the ZPL (marked by arrows). Two of these lines can even be identified within 1 s integration time in Fig. 1 (marked by arrows). The second series [Fig. 2(c)] was measured about 6.5 min after the first series. Here, for the first 30 s, the ZPL is nearly constant at $E_{ZPL} = 2.1178$ eV. Then an abrupt spectral shift occurs and the ZPL splits up into peaks with higher energy. The splitting can be explained by a rapid change (faster than t_{int}) between two metastable charge configurations in the surrounding of the NC, inducing different recombination energies via the Stark effect [21]. Such spectral shifts occur several times during this series. Most interestingly, the additional peaks below the ZPL can also be seen in this series, having fixed distances to the ZPL and thus shifting as the ZPL. The third series [Fig. 2(e)] was measured about 4.5 min after the second series. As a new feature, the NC changed into an *off* state after 78 s. At $t = 126$ s, the NC again changed into an *on* state. During the *off* state, also the additional lines disappear. Resuming Fig. 2, the stability of the NC emission enables the observation of new lines at fixed distance with respect to the ZPL.

In order to investigate these new lines in more detail, we energetically shifted single spectra showing only one ZPL

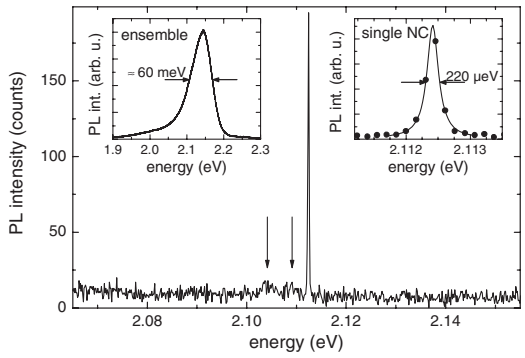

FIG. 1. PL spectrum of a single CdSe-CdS-ZnS NC embedded in a PEO matrix ($P_{exc} = 2.5$ mW, $t_{int} = 1$ s). Right inset: Lorentz fit of the ZPL. The line width of 220 μeV is limited by the resolution of the spectrometer. Left inset: PL spectrum of an ensemble of NCs before exchange of ligands.

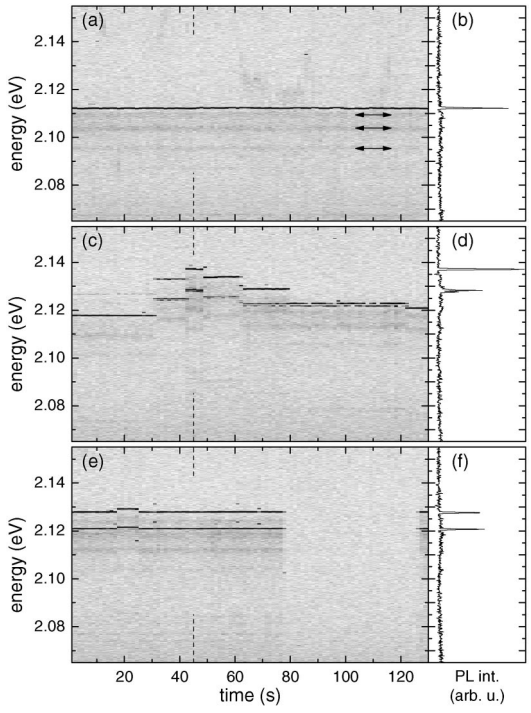

FIG. 2. Three series of PL spectra of the same NC as in Fig. 1. Each chart (a),(c),(e) shows 100 consecutively measured spectra ($P_{exc} = 2.5$ mW, $t_{int} = 1$ s, 0.3 s data procession time between each spectrum). The PL intensity is gray scaled where dark means a strong signal. The vertical (horizontal) axis gives the energy (time t). (b),(d),(f) show for each series a single spectrum obtained at $t = 45$ s [broken lines in (a),(c),(e)].

by setting E_{ZPL} to zero relative energy. The average of 81 of these shifted spectra are shown in Fig. 3(a). Most strikingly, in this depiction, several further peaks besides the ZPL can clearly be observed. These peaks are marked by arrows and labeled by characters A–I. For comparison, Fig. 3(b) shows an average of only 18 shifted single spectra which were obtained with $P_{exc} = 3.9$ mW instead of 2.5 mW as in (a). The intensities of the peaks roughly scale as the excitation power, since the intensity axis in (b) is scaled 3.9/2.5 times larger than in (a). The spectra of (b) were taken more than 30 min after the spectra of (a). In Fig. 3(b), the arrows are directly copied from (a); thus, all the features in (a) are reproduced in (b). Most of the peaks labeled in Fig. 3 can be assigned to phonon modes which couple to excitons leading to phonon replicas in the emission spectra, as will be shown in the following. Replica close to the ZPL are of special interest since they are assigned to discrete acoustic phonons and have not been previously reported for PL spectra of single NCs.

Acoustic phonons.—Confined acoustic phonons in NCs are discussed in literature [6–8,22], mostly based on Lamb's theory of a free homogeneous elastic body of spherical shape [16]. The acoustic vibrations fall into two categories: torsional and spheroidal modes. Former are transversal leading to vibrations without dilatation while the latter are in general both longitudinal and transversal leading to vibrations with dilatation. Each mode can be characterized by a radial mode number n and an angular mode number l. It has been shown that the interaction between carriers and acoustic phonons arises mainly via deformation potential coupling [23–26]. In spherical NCs the excitonic coupling to the breathing mode with $n = 0$ and $l = 0$ is reported to be dominant [23,26]. Like all modes with $l = 0$, this mode is purely longitudinal. Generally, the frequencies of longitudinal modes $\omega_{n0} = 2\pi\chi_{n0}v_L/R$ are according to Lamb determined by the solutions of the equation

$$\frac{\tan\chi_{n0}}{\chi_{n0}} = \left(1 - \frac{\chi_{n0}^2}{4}\frac{v_L^2}{v_T^2}\right)^{-1}. \quad (1)$$

Here, χ is a dimensionless variable, R is the radius of the NC and v_L (v_T) is the longitudinal (transversal) sound velocity inside the NC. The ratio v_L/v_T is about 2.3 for CdSe and differs only slightly in CdS and ZnS [27]. With that we obtain for the breathing mode and its two radial harmonics:

$$\omega_{00} = 2.86\frac{v_L}{R}, \qquad \omega_{10} = 6.16\frac{v_L}{R}, \qquad \omega_{20} = 9.34\frac{v_L}{R}. \quad (2)$$

In a first approximation, we neglect the different sound velocities of the thin shell material and assume that the sound velocities of the CdSe core are valid for the whole NC with a diameter of $2R = 4.7$ nm. With $v_L = 3.63 \times 10^5$ cm/s [27] we obtain 2.9 meV, 6.3 meV, and 9.6 meV for $\hbar\omega_{00}$, $\hbar\omega_{10}$, and $\hbar\omega_{20}$, respectively. These energies give the distance of corresponding phonon replica to the ZPL. We plotted the positions of the breathing mode replicas at the low-energy side of the ZPL as open circles in Fig. 3(a). There is a nice agreement of the calculated modes with the measured peaks B–D suggesting to assign peak B to the lowest breathing mode (ω_{00}) and the peaks C and D to its higher harmonics (ω_{10} and ω_{20}, respectively). It has been shown that low-lying vibrational modes of NCs can in good agreement be calculated within the above mentioned theory. Nevertheless, modeling a NC as a continuous elastic sphere with no dispersion of the acoustic phonons surely implies some inaccuracies, especially for higher modes with their wavelengths becoming comparable to the lattice constant of the NC. Qualitatively, the flattening of the phonon dispersion for increasing wave vectors implies a decrease of the wave velocity and should lead to a decrease of the energies of higher harmonics compared to the dispersionless model. In fact, the calculated energies in Fig. 3(a) are rather larger than smaller compared to the measured peaks.

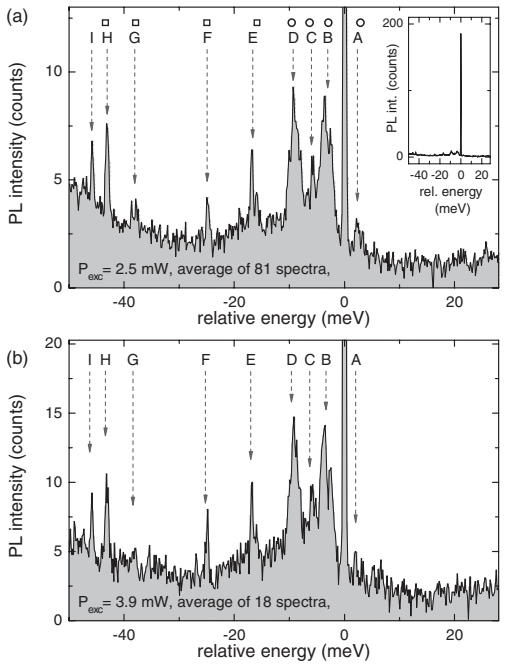

FIG. 3. (a) Average of 81 spectra, each obtained with $P_{exc} = 2.5$ mW and $t_{int} = 1$ s. Before averaging, each spectrum has been energetically shifted by setting E_{ZPL} to zero relative energy. Distinct peaks besides the ZPLs are marked by arrows and labeled by characters A–I. The squares give the energies of different phonons as reported in literature. The circles give calculated energies of confined acoustic phonons. The inset shows the whole averaged spectrum to compare the intensities of the ZPL and its neighboring peaks. (b) Similar spectrum as in (a), but here, the average is calculated from 18 single spectra obtained with $P_{exc} = 3.9$ mW.

The peaks B–E in Fig. 3 have different widths and especially peak B shows a fine structure (close to the resolution limit). Both features cannot be fully explained by now. In this context, it might be important, that besides the breathing modes a wealth of other vibrational modes exist inside the NC. The lowest lying spheroidal (torsional) mode can be calculated to $\hbar\omega_{02} = 1.20$ meV (1.15 meV). One may speculate that other vibrational modes lead to a broadening of the breathing modes.

Trying to assign peak A, one might think of a replica being generated by annihilation of an acoustic phonon; however, its energy is smaller than the calculated energy of the breathing mode, which is also depicted in Fig. 3. Thus the origin of peak A is not unambiguously clear.

The phonon dispersion of wurtzite CdSe has been investigated in Ref. [28], where the measured value of the backfolded LA phonon at the Γ point of the Brillouin zone is given as $\hbar\omega_{\mathrm{LA}} = 14.4$ meV. This suggests to identify peak E, which occurs at about -16.7 meV together with a shoulder at -16.0 meV, as a LA phonon replica. Deviations from the reported energies may arise since we deal with a NC at $T = 8$ K instead of bulk material at room temperature as in Ref. [28].

Optical phonons.—Peak F at a relative energy of -25.0 meV can be identified as the LO phonon replica of the CdSe core of our core-shell-shell NC. Such LO phonon replica from the core of a single NC are well known. For a single CdSe NC (no core-shell system) with a diameter of 4.5 nm a value of -25.6 meV has been reported [3], which is depicted as a square in Fig. 3(a), for comparison. Peak G at -37.9 meV can be identified as the LO phonon replica of the CdS shell material. The LO phonon energy of CdS has been reported to be about 37.8 meV [square in Fig. 3(a)], measured by Raman spectroscopy in both, bulk [27] and ensembles of CdS NCs [29]. Peak H at -43.2 meV can be assigned to the LO phonon replica of the outer shell of our NC. In CdSe-ZnS core-shell NCs, the LO phonon energy of the ZnS shell observed by Raman spectroscopy on an ensemble of NCs has been reported to be about 43.4 meV [square in Fig. 3(a)] [30]. The observation of LO phonon replica of the shells in the PL spectra of a single NC is quite remarkable, because of the small thickness of the shells of 1 ML or less. At last, in Fig. 3, we observe peak I at a relative energy of -45.8 meV, which we cannot identify, yet.

In summary, we investigated single highly luminescent CdSe-CdS-ZnS core-shell-shell NCs whose ligands were exchanged to PEO before they were embedded in a PEO matrix. By averaging PL spectra of a single NC, we were able to observe a set of peaks with distinct distances to the ZPL on its low-energy side. These peaks are attributed to phonon replicas. Most importantly, modeling the NC as an elastic sphere reveals that three peaks close to the ZPL are arising due to the breathing mode and its two radial harmonics. Other peaks were assigned to LA and LO phonons of the CdSe core and LO phonons of both the CdS and ZnS shells.

We gratefully acknowledge financial support of the Deutsche Forschungsgemeinschaft via the SFB 508 ''Quantum Materials'' and the Graduiertenkolleg 1286.

*tkipp@physnet.uni-hamburg.de

[1] M. Hines and P. Guyot-Sionnest, J. Phys. Chem. **100**, 468 (1996).
[2] D. Talapin *et al.*, Nano Lett. **1**, 207 (2001).
[3] S. A. Empedocles, D. J. Norris, and M. G. Bawendi, Phys. Rev. Lett. **77**, 3873 (1996).
[4] S. A. Empedocles *et al.*, Adv. Mater. **11**, 1243 (1999).
[5] E. Duval, A. Boukenter, and B. Champagnon, Phys. Rev. Lett. **56**, 2052 (1986).
[6] A. Tanaka, S. Onari, and T. Arai, Phys. Rev. B **56**, 9977(E) (1997); Phys. Rev. B **47**, 1237 (1993).
[7] L. Saviot *et al.*, J. Non-Cryst. Solids **197**, 238 (1996).
[8] H. K. Yadav *et al.*, Phys. Rev. Lett. **98**, 029902(E) (2007); Phys. Rev. Lett. **97**, 085502 (2006).
[9] S. Okamoto and Y. Masumoto, J. Lumin. **64**, 253 (1995).
[10] J. Zhao and Y. Masumoto, Phys. Rev. B **60**, 4481 (1999).
[11] P. Palinginis and H. Wang, Appl. Phys. Lett. **78**, 1541 (2001).
[12] U. Woggon *et al.*, Phys. Rev. B **54**, 1506 (1996).
[13] T. D. Krauss and F. W. Wise, Phys. Rev. Lett. **79**, 5102 (1997).
[14] G. Cerullo, S. De Silvestri, and U. Banin, Phys. Rev. B **60**, 1928 (1999).
[15] M. Ikezawa *et al.*, Phys. Rev. B **64**, 201315(R) (2001).
[16] H. Lamb, Proc. London Math. Soc. 13, 187 (1882).
[17] I. Mekis *et al.*, J. Phys. Chem. B **107**, 7454 (2003).
[18] D. Talapin *et al.*, J. Phys. Chem. B **108**, 18826 (2004).
[19] W. Yu *et al.*, Chem. Mater. **15**, 2854 (2003).
[20] M. S. Nikolic *et al.*, Angew. Chem., Int. Ed. **45**, 6577 (2006).
[21] Y. Shen *et al.*, Phys. Rev. B **76**, 085312 (2007).
[22] A. Tamura, K. Higeta, and T. Ichinokawa, J. Phys. C **15**, 4975 (1982).
[23] S. Nomura and T. Kobayash, Solid State Commun. **82**, 335 (1992).
[24] T. Takagahara, Phys. Rev. Lett. **71**, 3577 (1993).
[25] A. M. Alcalde *et al.*, Solid State Commun. **116**, 247 (2000).
[26] M. R. Salvador, M. W. Graham, and G. D. Scholes, J. Chem. Phys. **125**, 184709 (2006).
[27] *II–VI and I–VII Compounds; Semimagnetic Compounds*, edited by U. Rössler, Landolt-Börnstein—Group III Condensed Matter, Vol 41B (Springer, New York, 1999).
[28] F. Widulle *et al.*, Physica (Amsterdam) **263–264B**, 448 (1999).
[29] J. J. Shiang, S. H. Risbud, and A. P. Alivisatos, J. Chem. Phys. **98**, 8432 (1993).
[30] A. V. Baranov *et al.*, Phys. Rev. B **68**, 165306 (2003).